Available online at www.sciencedirect.com
SCIENCE DIRECT®
Medical Engineering & Physics 27 (2005) 13–18
Medical Engineering & Physics
www.elsevier.com/locate/medengphy

A predictive study of the mechanical behaviour of coronary stents by computer modelling

Francesco Migliavacca[a,*], Lorenza Petrini[b], Valeria Montanari[a], Isabella Quagliana[a], Ferdinando Auricchio[b], Gabriele Dubini[a]

[a] *Laboratory of Biological Structure Mechanics, Bioengineering and Structural Engineering Department, Politecnico di Milano, Piazza Leonardo da Vinci, 32, 20133 Milan, Italy*
[b] *Department of Structural Mechanics, Università degli Studi di Pavia, Pavia, Italy*

Received 3 November 2003; received in revised form 22 July 2004; accepted 16 August 2004

Abstract

Intravascular stents are small tube-like structures expanded into stenotic arteries to restore blood flow perfusion to the downstream tissues. The stent expansion is an important factor to define the effectiveness of the surgical procedure: it depends on the stent geometry and includes large displacements and deformations, geometric and material non-linearity. Numerical analyses seem appropriate to study such a complex behaviour after a free stent expansion. In this study the finite element method (FEM) was applied to a new generation coronary stent. Results from computations were compared with those from a laboratory experiment in terms of radial expansion and elastic recoil. By means of a scanning electronic microscopy the area of plastic deformation were also detected and compared with those obtained in the numerical simulation. Matching between the different measurements was quite satisfactory even if some discrepancies were present due to the absence of the balloon in the numerical model.

Keywords: Finite element method; Experimental test; Mechanical properties; Coronary stent

1. Introduction

Stents typically are tiny wire mesh tubes used to open arteries that have become clogged by the build-up over time of fat, cholesterol or other substances. The stent is collapsed to a small diameter, placed over an angioplasty balloon catheter and moved into the area of the blockage. When the balloon is inflated, the stent expands and deforms plastically, locks in place and forms a scaffold to hold the artery open. Currently balloon-expanding available stents are made from medical grade stainless steel.

Today's device manufacturers use a variety of experimental tests [1–6] to ensure that stents have accurate properties. However, the small and complex geometry of the stent often does not allow to carry out all the tests usually required for a standard medical device. For example, strains cannot be measured easily in a structure like a stent. In this regards computational analyses, based for example on the finite element method (FEM) can be adopted. In the literature there are computational studies [7–11] on the optimisation of the stent mechanical properties, which can surely lead to a better long-term efficacy of the device itself. Indeed, computational analyses could provide access to an extensive amount of information under highly controlled conditions, thus, making it possible to screen different and competing coronary stent design alternatives prior to costly prototype fabrication. On the other hand, due to the lack of sophisticated and often ad hoc numerical methods capable of handling the complexity of real-life stent behaviour, up to now designers have only used computational analyses after prototype fabrication to provide further understanding of typical stent performance. Therefore, a critical requirement for a numerical code, which is necessary to reach its full potential with regards to the stent

* Corresponding author. Tel.: +39 02 2399 4283; fax: +39 02 2399 4286.
E-mail address: francesco.migliavacca@polimi.it (F. Migliavacca).

1350-4533/$ – see front matter © 2004 IPEM. Published by Elsevier Ltd. All rights reserved.
doi:10.1016/j.medengphy.2004.08.012

simulation, is the development of accurate and efficient algorithms capable of simulating the real stent expansion, recoil, flexibility, interaction with the vascular wall, etc.

This study aims to show how some mechanical properties of a new generation balloon-expanding stent can be studied accurately with computational analyses based on the FEM. The numerical results are compared with an experimental test.

2. Material and method

2.1. Computational simulation

The selected stent is the 'Cordis BX Velocity' (Johnson & Johnson Interventional System, Warren, NJ, USA). Using a Nikon SMZ800 stereo microscope (Nikon Corporation, Tokyo, Japan) the main stent dimensions were extracted and used to build a 3D CAD model of the undeformed shape of the stent (Fig. 1) by means of the commercial software Rhinoceros 1.1 Evaluation (Robert McNeel & Associates, Indianapolis, IN, USA). The model is characterized by rings connected at the top by six links. The inner diameter in the unexpanded configuration is 0.9 mm while the thickness of the stent is 0.14 mm. This configuration is, in the reality, 'deformed' as the stent was crimped on the delivery system. This feature is considered in the selection of the material characteristics. Indeed, the stent is made of AISI 316L stainless steel. The inelastic constitutive response is described through a von Mises–Hill plasticity model with hardening. The Young modulus is 196 GPa, the Poisson ratio 0.3, the yield stress 205 MPa [8]. Using a kinematic hardening the yield stress was reduced to 105 MPa to take into account the crimping.

The model was meshed with 10-node tetrahedral elements. The number of nodes was 153199, while that of elements was 69593, selected after a sensitivity analysis. Element skewness was always smaller than 0.90. The mesh was automatically generated by GAMBIT commercial code (Fluent Inc., Lebanon, NH, USA).

A large deformation analysis is performed using ABAQUS commercial code (Hibbit Karlsson & Sorenses Inc., Pawtucket, RI, USA) based on the finite element method. In particular, the ABAQUS/Standard program is used in the classical displacement formulation. The nonlinear problem, due to material plasticity and contact constraint, is solved using a Newton–Raphson's method. The method convergence criterion consists of ensuring that the largest residual in the balance equations and the largest correction to any nodal unknown provided by the current Newton iteration are sufficiently small. In particular, for the studied problem the convergence is verified when the residual force is less than a predefined tolerance (in our case 0.5% of the average force in the structure, averaged over space and time) and when the largest displacement correction is less than a predefined tolerance (in our case 10% of the largest incremental displacement).

The numerical simulation was performed to mimic the free expansion of the stent. A uniform linearly increasing radial pressure (P) was applied at the internal surface of the stent till the value of 1.2 MPa.

The simulation was performed to investigate also the mechanical properties of the stent after the load removal. The stent was unloaded decreasing the internal pressure up to zero. The following quantities were calculated:

$$\text{distal radial recoil} = \frac{R_{\text{distal}}^{\text{load}} - R_{\text{distal}}^{\text{unload}}}{R_{\text{distal}}^{\text{load}}}$$

$$\text{central radial recoil} = \frac{R_{\text{central}}^{\text{load}} - R_{\text{central}}^{\text{unload}}}{R_{\text{central}}^{\text{load}}}$$

$$\text{longitudinal recoil} = \frac{L^{\text{load}} - L^{\text{unload}}}{L^{\text{load}}}$$

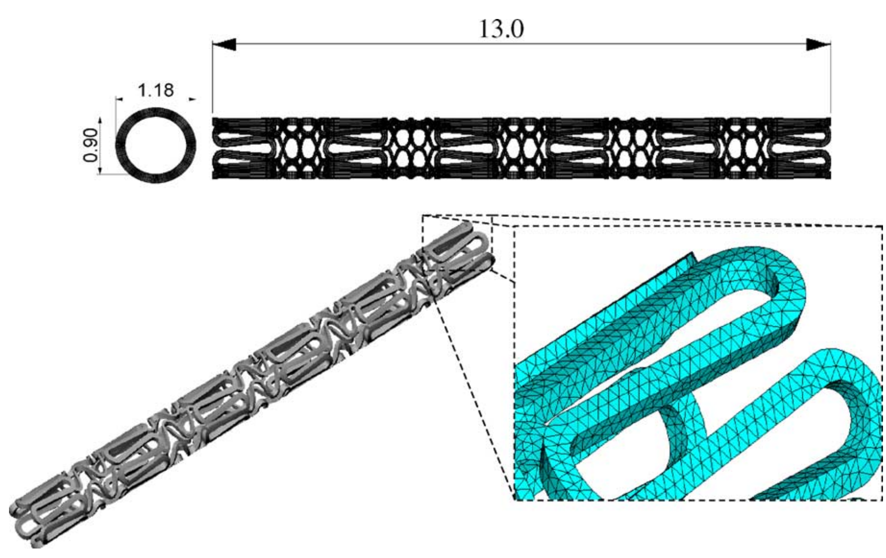

Fig. 1. 3D CAD model of the 'Cordis BX Velocity' stent. In the inset is depicted a particular of the mesh.

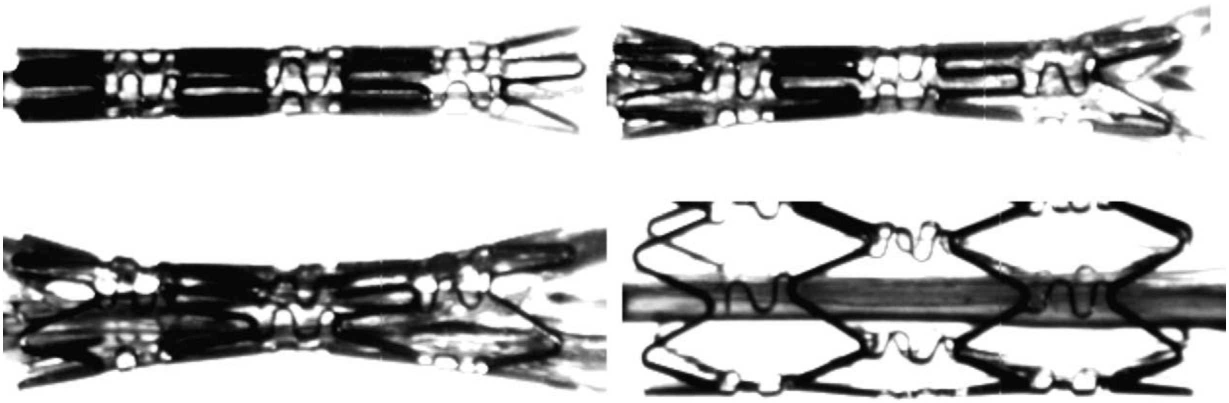

Fig. 2. Stent expansion as acquired by the optic estensometer at four different inflating pressures. It is possible to observe the expansion of the balloon in the distal zones of the stent before a uniform shape is reached.

$$\text{foreshortening} = \frac{L - L^{\text{load}}}{L}$$

$$\text{dogboning} = \frac{R^{\text{load}}_{\text{distal}} - R^{\text{load}}_{\text{central}}}{R^{\text{load}}_{\text{distal}}}$$

where L^{load}, $R^{\text{load}}_{\text{central}}$ and $R^{\text{load}}_{\text{distal}}$ are the longitudinal length, the central radius and the distal radius, respectively, after the load application, while L^{unload}, $R^{\text{unload}}_{\text{central}}$ and $R^{\text{unload}}_{\text{distal}}$ are the same quantities when the load is removed. L is the initial length of the stent.

2.2. Experimental test

An optic estensometer VE500 (Trio Sistemi e Misure S.r.l., Dalmine, Italy) was adopted to measure the expansion of the 'Cordis BX Velocity' stent. After a proper calibration the measurement of the central diameter of the stent was obtained by elaborating the acquired image. The inflating pressure was obtained by means of a manual pump similar to those used in clinical practice. The balloon was inflated at increasing pressures till the value of 1.2 MPa and the corresponding stent diameters were measured. Fig. 2 reports four different instants of the inflating process. Plastic deformations are expected and for this reason after the deployment, the stent was inspected by scanning electronic microscopy (SEM).

3. Results and discussion

3.1. Computational model

Fig. 3 depicts the von Mises stresses at the inflating pressure of 0.5 MPa and the equivalent plastic deformations after the load removal. More interesting is the relation between the central diameter and the inflating pressure. Fig. 4 demon-

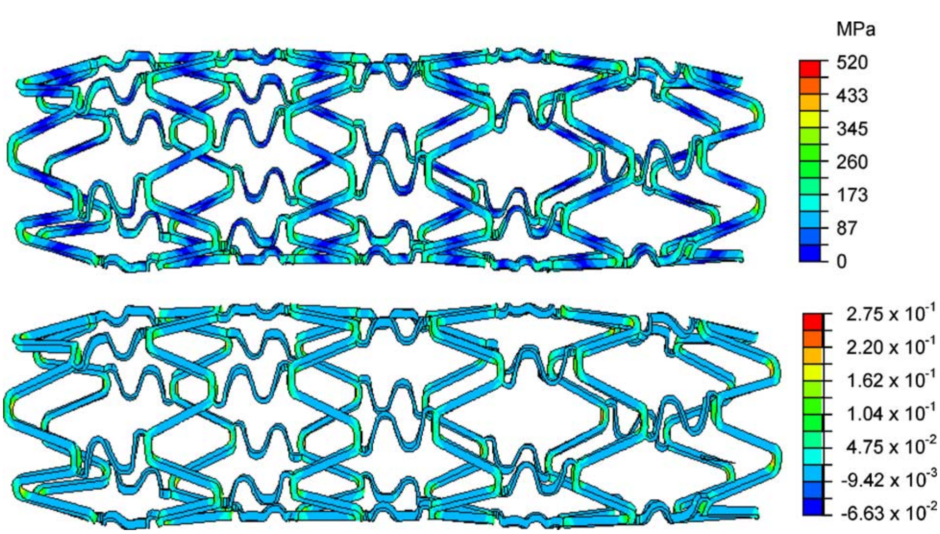

Fig. 3. von Mises stresses at the inflating pressure of 0.5 MPa (top) and equivalent plastic deformation after the load removal (bottom).

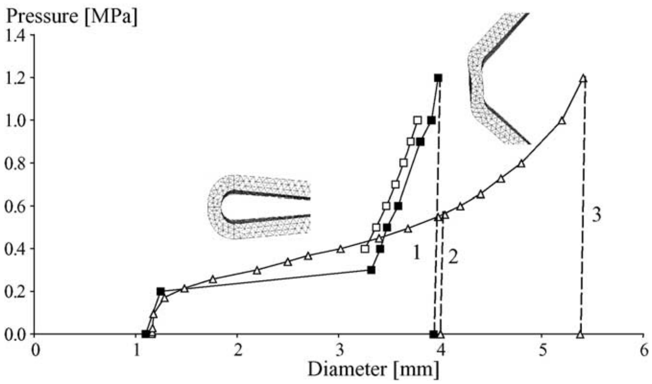

Fig. 4. Results from the FEM analysis (empty triangle), from the experimental test (solid squares) and data provided by the company (empty squares). The dotted lines represent the unload history at different values of inflating pressures both for the FEM and the experimental analyses. It should be noted that at 0.5 MPa the diameter reached by the stent is similar in the FEM simulation and the experimental test.

Table 1
Main quantities of interest of the FEM model of the stent measured after the load removal of 0.5 MPa, values at which the stent reaches its nominal value

Quantity	Percentage value (%)
Distal elastic recoil ($L = 0$ mm)	1.16
Distal elastic recoil ($L = 13$ mm)	1.10
Central elastic recoil	1.18
Longitudinal recoil	−0.13
Foreshortening	8.22
Dogboning ($L = 0$ mm)	−29.5
Dogboning ($L = 13$ mm)	−23.3

$L = 0$ mm: proximal part of the stent; $L = 13$ mm: distal part of the stent.

strates that when the inflating pressure reaches the value of 0.2 MPa the stent expands rapidly. At higher pressures the increment in the diameter is less pronounced. This behaviour can be explained observing that the rings of the stent behave as a cantilever under flexion (Fig. 5a): the structure undergoes large deformations with small applied pressure. The behaviour at higher pressures can be explained observing that the rings now resemble to narrow beams subjected to tensile axial load (Fig. 5b) showing an increased stiffness with respect to the initial configuration. Table 1 reports the main quantities of interest following a load removal after a 0.5 MPa load. The foreshortening is remarkable, the radial elastic recoil is minimal along the stent, while the dogboning (i.e. flaring of stent ends) shows negative values, which means that there is not an over dilatation of the distal parts of the stent. This fact is extremely important during the stent expansion to minimise dissections or damage to the intimal layer of the vessel.

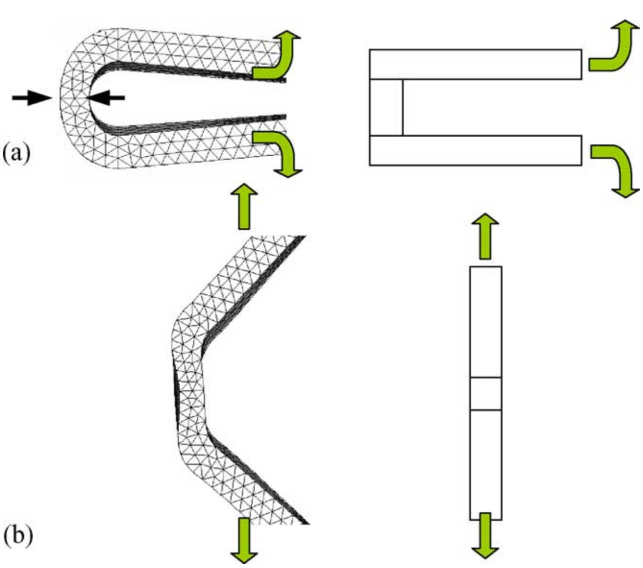

Fig. 5. Sketch of the ring stent like a cantilever under flexion before the expansion (a) and like beam subjected to tensile load after the expansion (b).

3.2. Experimental test

The inflating pressure–internal diameter relationship supplied by the company manufacturing the stent is reported in Fig. 4 together with the same curve obtained from our experiment. The similarity between the two experimental curves is very good, even if our experimental curve overestimates slightly the diameter reached by the stent. Furthermore, the first part of the expansion is similar to that provided by the computational simulation. A discrepancy can be deducted at high pressure levels. The behaviour of the stent in the computational simulation is not descriptive of the real situation.

An interesting observation can be done calculating the central radial elastic recoil in the experimental test after the removal of 1.2 MPa (Fig. 4, line 1) and those obtained removing the load in the FEM simulation at the same expanded diameter when the inflating pressure is 0.5 MPa (Fig. 4, line 2) or at the same inflating pressure (Fig. 4, line 3). Indeed the experimental central radial recoil was 1.1%, while those from FEM simulations were 1.2 and 0.59% at the same diameter and at the same maximum inflating pressure, respectively. Increasing the inflating pressure, the recoil decreases due to the non linearity of the material. From this considerations we conclude that the second part of the inflating pressure–internal diameter curve is not representative of the reality due to the absence of the balloon which limits the free expansion of the stent. The value of 0.5 MPa was hence selected as representative for the comparison between the computational and the experimental tests.

Regarding the deformations in the stent, the SEM analysis (Fig. 6) made possible the detection of the Luders lines (i.e. elongated surface markings or depressions caused by localised plastic deformation that results from discontinuous or inhomogeneous yielding). Indeed, in accordance with this observation the computational simulation at 0.5 MPa shows in this area the higher equivalent plastic deformation.

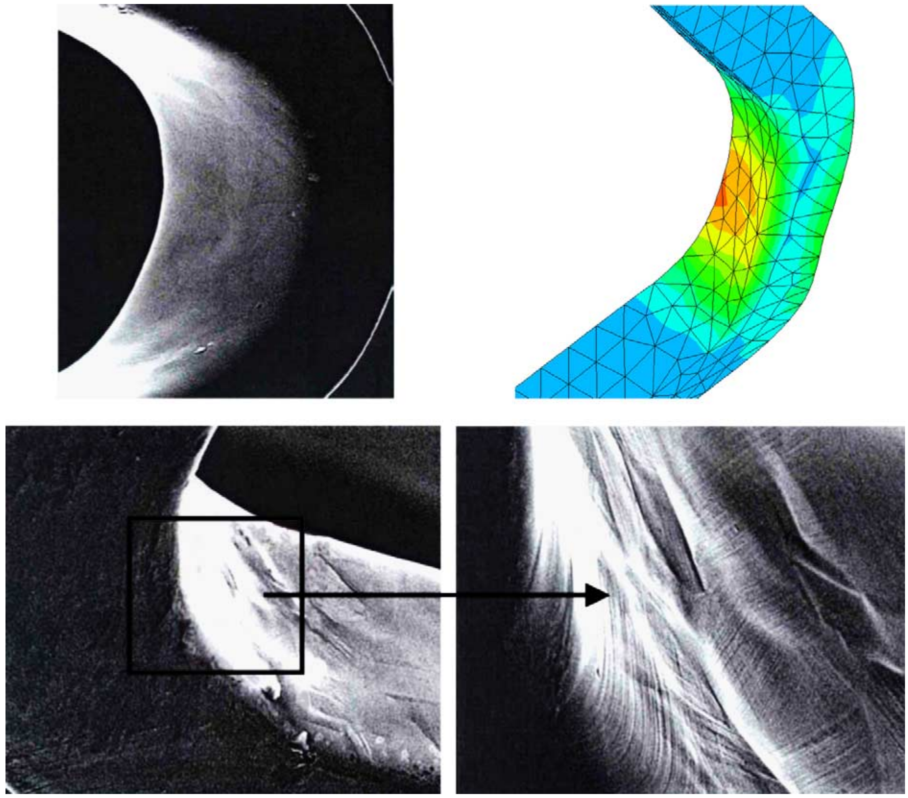

Fig. 6. Scanning electron microscopy (SEM) images and equivalent plastic deformation in the corresponding area of the FEM model. The enlargement in the area of the link shows clearly the areas of plastic deformation (Luders lines).

4. Conclusions

From the computational simulation the following results were obtained:

(i) a lower value of the yield stress representative of the crimping of the stent on the delivery system (balloon plus catether) allowed to have an initial expansion similar to the experimental one as shown in Fig. 4;
(ii) the absence of any balloon model is the real decisive element in interpreting the discrepancies between the experimental and the computational tests. Indeed, once the balloon is expanded, its presence cannot be neglected and the inflating pressure is not transmitted proportionally to the stent;
(iii) once the balloon reaches its nominal diameter, the stress field in the stent can be compared with the experimental one at the same expanded diameter and not at the same inflating pressure.

Only a very complex computational model accounting for the angioplasty balloon and the interaction with the stent would reproduce correctly the free expansion of the stent. In this regards, efforts have recently appeared in the literature to study the angioplasty and stenting procedures by means of computational structural analysis [8,11–17]. The stent–artery interaction is investigated to evaluate the vascular stress state induced by the stent struts [17] and the tissue prolapse within the stent struts [11]. The work by Holzapfel et al. [16] is one of the most exhaustive on the subject and we refer the reader to such a reference since it also contains a brief review of the quoted studies.

References

[1] Duda SH, Wiskirchen J, Tepe G, Bitzer M, Kaulich TW, Stoeckel D, et al. Physical properties of endovascular stents: an experimental comparison. J Vasc Interv Radiol 2000;115:645–54.
[2] Dyet JF, Watts WG, Ettles DF, Nicholson AA. Mechanical properties of metallic stents: how do these properties influence the choice of stent for specific lesions? Cardiovasc Interv Radiol 2000;23:47–54.
[3] Etave F, Finet G, Boivin M, Boyer JC, Rioufol G, Thollet G. Mechanical properties of coronary stents determined by using finite element analysis. J Biomech 2001;34:1065–75.
[4] Flueckiger F, Sternthal H, Klein GE, Aschauer M, Szolar D, Kleinhappl G. Strength, elasticity, and plasticity of expandable metal stents: in vitro studies with three types of stress. J Vasc Interv Radiol 1994;5:745–50.
[5] Ormiston JA, Ruygrok PN, Webster MW, Stewart JT, White HD. Mechanical properties of five long stents compared. J Invasive Cardiol 1998;10(Suppl B):35B.
[6] Ormiston JA, Dixon SR, Webster MW, Ruygrok PN, Stewart JT, Minchington I, et al. Stent longitudinal flexibility: a comparison of 13 stent designs before and after balloon expansion. Catheter Cardiovas Interv 2000;50:120–4.

[7] Dumoulin C, Cochelin B. Mechanical behaviour modelling of balloon-expandable stents. J Biomech 2000;33:1461–70.
[8] Auricchio F, Di Loreto M, Sacco E. Finite-element analysis of a stenotic artery revascularization through a stent insertion. Comp Meth Biomech Biomed Eng 2001;4:249–63.
[9] Tan LB, Webb DC, Kormi K, Al-Hassani ST. A method for investigating the mechanical properties of intracoronary stents using finite element numerical simulation. Int J Cardiol 2001;78:51–67.
[10] Migliavacca F, Petrini L, Colombo M, Auricchio F, Pietrabissa R. Mechanical behaviour of coronary stents investigated through the finite element method. J Biomech 2002;35:803–11.
[11] Prendergast PJ, Lally C, Daly S, Reid AJ, Lee TC, Quinn D, et al. Analysis of prolapse in cardiovascular stents: a constitutive equation for vascular tissue and finite element modelling. J Biomech Eng 2003;125:692–9.
[12] Lee RT, Loree HM, Cheng GC, Lieberman EH, Jaramillo N, Schoen FJ. Computational structural analysis based on intravascular ultrasound imaging before in vitro angioplasty: prediction of plaque fracture locations. J Am Coll Cardiol 1993;21:777–82.
[13] Oh S, Kleinberger M, McElhaney JH. Finite-element analysis of balloon angioplasty. Med Biol Eng Comput 1994;32: S108–14.
[14] Rogers C, Tseng DY, Squere JC, Edelman ER. Balloon–artery interactions during stent placement. A finite element analysis approach to pressure, compliance, and stent design as contributors to vascular injury. Circ Res 1999;84:378–83.
[15] Gourisankaran V, Sharma MG. The finite-element analysis of stresses in atherosclerotic arteries during balloon angioplasty. Crit Rev Biomed Eng 2000;8:47–51.
[16] Holzapfel GA, Stadler M, Schulze-Bauer CAJ. A layer-specific 3D model for the simulation of balloon angioplasty using magnetic resonance imaging and mechanical testing. Ann Biomed Eng 2002;30:753–67.
[17] Migliavacca F, Petrini L, Massarotti P, Schievano S, Auricchio F, Dubini G. Stainless and shape memory alloy coronary stents: a computational study on the interaction with the vascular wall. Biomech Model Mechanobiol 2004;2:205–17.